2017 21st International Conference on Process Control (PC)
June 6–9, 2017, Štrbské Pleso, Slovakia

Modelling of Hybrid CSTR Plant: Heat Transfer Considerations

Piotr Laszczyk, Malgorzata Niedzwiedz, Piotr Skupin, Mieczyslaw Metzger
Faculty of Automatic Control, Electronics and Computer Science
Silesian University of Technology, Gliwice, Poland
{piotr.laszczyk, malgorzata.niedzwiedz, piotr.skupin, mieczyslaw.metzger}@polsl.pl

***Abstract*—The continuously stirred tank reactor (CSTR) may exhibit various nonlinear effects, for example, multi-stability or sustained oscillations. This makes the CSTR one of the most difficult industrial units for control and the system instability or thermal runaway indicate that the safety issues must also be taken into account. In comparison to the real reactor, a hybrid system is safe and less expensive alternative for testing new concepts in control. In this paper, we consider a hybrid reactor that consist of a jacketed vessel and LabVIEW based real-time simulator of a chemical reaction. To make the hybrid reactor a highly nonlinear benchmark plant, the system parameters must be carefully selected. Instead of making time consuming experiments, the preliminary simulation tests would be helpful in selection of the process parameters. For this purpose three models of various complexity for the real hybrid reactor are developed. We show that an overall heat transfer coefficient cannot be assumed constant to obtain a good agreement between the simulation results and the measurement data. The paper also presents the influence of the coefficient on the dynamical behavior of the hybrid reactor based on the bifurcation analysis.**

Keywords—heat transfer process; partially simulated chemical reactor; modelling and simulation; bifurcation analysis

I. INTRODUCTION

Rapid development of technology made the implementation of new ideas in the control field possible. Therefore, a vast range of research in the second half of the 20th century was devoted to the control of chemical reactors [1,2,3,4]. One of the most promising methods is the model based control that incorporates the dynamic model of a given process into the control algorithm. Since that time, several nonlinear model based control algorithms have been proposed: PMBC [5,6], linearizing control [7,8], generic model control (GMC) [9] and predictive functional control (PFC) [10,11]. However, the implementation of the model-based algorithms in control equipment is a still demanding task due to limited computational power and is still under study [12,13,14,15,16].

The main goal in controlling a chemical reactor is to meet required selectiveness with high production rate. At the same time, safety issues in the process should be taken into account. Those objectives cannot be achieved without controlling the temperature inside the reactor vessel. Usually, the temperature is controlled by changing the flow rate of coolant in the reactor jacket. However, nonlinear and sometimes unstable characteristics makes a chemical reactor one of the most difficult industrial units for control. For example, the thermal runaway scenarios in a chemical plant can be related to conditions in which the heat generation of an ongoing reaction exceeds the heat dissipation capacity of the process equipment. Thus, testing new control algorithms with a real reactor unit is associated with the risk of explosion and is often expensive.

One of the possible ways that allows safer and inexpensive testing of new control algorithms is to use numerical simulators. However, reliability of obtained results strongly depends on the quality of model used in simulations. Another possibility to make results of such tests more reliable is to use a hybrid reactor. In such case, the reaction is simulated using well-known mathematical models derived from mass and energy balances. At the same time, the heat transfer phenomena are not simulated but occur in the real part of the system, i.e., inside the reactor vessel and the reactor jacket. The heat of reaction is simulated using a heating device inside the reactor vessel and the amount of heat released during the reaction is determined by the mathematical model of the system. The advantage of the approach is that the control system operates on real actuators and uses the measurement data acquired from real sensors and transducers. In some cases, the sensors dynamics is considered as relevant for control tasks in chemical and biological reactors [17,18].

Originally the idea of the hybrid chemical reactor, called also partially simulated reactor, arose in 1965 [19]. In the proposed setup, the reaction heat was produced using steam heaters. Later works extended the idea by using the direct steam injection into the reactor [20,21,22] or steam heater [23]. Other hybrid reactors were equipped with electric heaters placed inside the reactor vessel [24,25,26,27]. In all the mentioned cases, the hybrid reactor was considered as a highly nonlinear plant for testing new concepts in control. However, none of these papers shows that the hybrid system exhibited nonlinear phenomena, such as multiplicity of steady states or limit cycles. Hence, one of the main goals in designing the hybrid reactor is to ensure the possibility of observing the mentioned nonlinear effects. This can be achieved by a proper selection of the reaction parameters and input process values (flow rates, inlet concentration and temperatures). One should also take into account that the existence of the desired reactor behavior for a given reaction parameters strongly depends on the technological limitations (e.g., mixing efficiency, heat removal effectiveness). Selection of proper reaction parameters is difficult in the analytical way because of implicit mathematical relations describing chemical reaction and heat transfer phenomena. One of the options is the selection made

by experiments based on trial and error method, but this can be a time consuming process. Therefore, we propose to perform preliminary tests by making numerical simulations. For this purpose, we derive a model of the real part of the hybrid reactor that is able to capture the heat phenomena inside the reactor vessel and jacket. The derivation of the model and its validation is the main goal of this paper.

II. Plant Description

The experimental setup with the hybrid reactor (Fig. 1) is the continuation of the research presented in [25].The hybrid CSTR consists of two concentric vertical cylinders (Fig.1). The reactor vessel (inner cylinder) is made of 2 mm thick stainless steel and has a volume V= 8.74 [L]. The vessel is surrounded by the jacket (outer cylinder) made of 5 mm thick PMMA. A cooling water flows through annular duct, which is formed by the space (volume V_j=2.06 [L]) between the inner and outer cylinder. The tap water enters at the bottom of the vessel and jacket and flows upward. A circulating pump is used to agitate the content of the vessel. The electromagnetic flow meters are used to measure volumetric flow rate through the vessel (F) and through the jacket (F_j), and the flow rates are controlled by two additional local PI controllers (R_1, R_2) with independent control valves (V_1, V_2). The input and output temperatures, and the ambient temperature are measured by means of Pt100 sensors. The reactor is equipped with an electric heater immersed in the water inside the reactor vessel. This heater is used to simulate the reaction heat. The chemical reaction with intentionally selected kinetic parameters is numerically simulated in LabVIEW. The measured temperature in the reactor vessel T_{out} and the flow rate F are supplied to the simulator. The simulator calculates the concentration c_A of substrate for a given input concentration c_{Ain} and the amount of heat E_r released in the reaction. Then, the calculated reaction heat E_r is a setpoint for additional local PI control loop (R_E) that maintains the power of the electric heater at the level E_r, irrespective of the voltage fluctuations. The amount of heat produced by the electric heater is measured by the active power meter (W). Analysis of PI control loops (R_1, R_2, R_E) performance showed their acceptable quality. Any small variability are practically dumped in the technological setup. This property is a result of long substitute time constants (few or even several minutes) which could be evaluated as a flow rate to volume ratio.

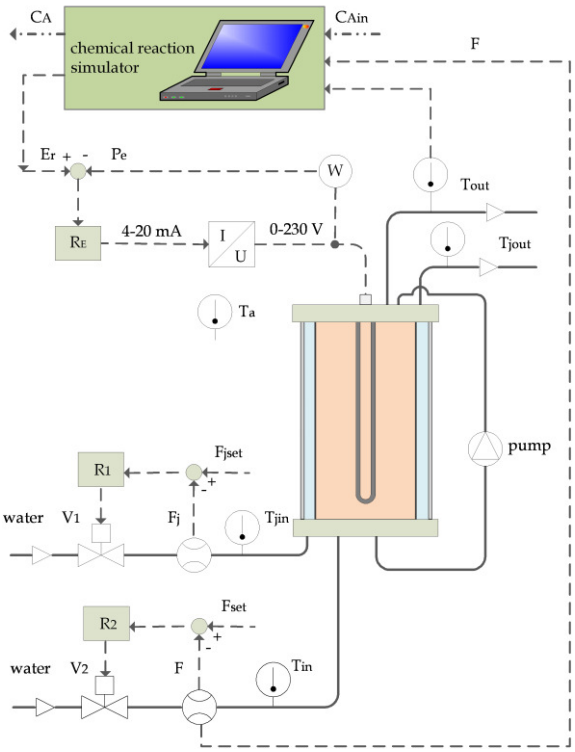

Fig. 1. The scheme of the hybrid CSTR plant

III. Modelling of the Hybrid Reactor

The mathematical model of the hybrid reactor setup must reflect its steady-state and dynamical behavior. The simplest form of the jacketed reactor model assumes that the reactor content as well as the coolant in the jacket are well-mixed. This assumption was adopted in modeling and simulation of hybrid chemical reactors in many other research works as well [19, 23, 27, 28, 29]. Based on energy and mass balances for the hybrid reactor, the lumped parameter model can be described by the following equations:

$$c_p \rho V \frac{dT}{dt} = c_p \rho F (T_{in} - T) - UA(T - T_j) + E_r , \qquad (1)$$

$$c_{pj} \rho_j V_j \frac{dT_j}{dt} = c_{pj} \rho_j F_j (T_{jin} - T_j) + UA(T - T_j) , \qquad (2)$$

where: c_p, c_{pj} –specific heat of the fluid inside the reactor and jacket [kJ/kg/K], respectively; ρ, ρ_j – density of the fluid inside the reactor and jacket [kg/L], respectively; V – reactor vessel volume [L]; V_j – jacket volume [L]; T, T_j – temperatures inside the reactor vessel and jacket [K], respectively; F, F_j – flow rates through the reactor vessel and jacket [L/min], respectively; UA – the overall heat transfer coefficient [kJ/min/K]; E_r=(–ΔH)·V·r – the reaction heat [kJ/min]; (–ΔH) – enthalpy of the reaction [kJ/mol]; r – reaction rate [mol/L/min]. In the remainder of the paper c_p=c_{pj} and ρ=ρ_j, since the real hybrid reactor is filled and cooled by water.

We further assume that the exothermic reaction $A \rightarrow B$ is of the first order and the product B do not influence the reaction rate. Hence, the reaction rate can be described by the well-known Arrhenius equation. The mass balance for the substrate A leads us to the following equations:

$$V \frac{dc_A}{dt} = F(c_{Ain} - c_A) - r \cdot V , \qquad (3)$$

$$r = k_0 \cdot \exp\left(-\frac{E}{R \cdot T}\right) \cdot c_A , \qquad (4)$$

where: c_{Ain}, c_A – substrate concentrations in the input and output [mol/L], respectively; E – activation energy [kJ/mol]; R – gas constant [kJ/mol/K]; k_0 – pre-exponential Arrhenius factor [1/min]. The reaction parameters k_0, E and ΔH are chosen intentionally to obtain required dynamic and static properties of the system.

The equations (1)-(4) describe the classical CSTR system and the obtained model will be referred to as the model 1. The unknown parameter UA can be estimated for the steady-state conditions based on the experimental data, collected for various flow rates F, F_j and heating power E_r. For identification purposes of heat transfer parameters the value of E_r was set in steps manually. By setting the derivatives in (1) and (2) equal to zero, one can find the equilibrium point:

$$T_0 = \frac{\left(\rho c_w (T_{jin} F_j + T_{in} F) + E_r\right) \cdot UA + \rho c_w F_j (T_{jin} \rho c_w F + E_r)}{\rho c_w (F_j + F) UA + \rho^2 c_w^2 F F_j}, \quad (5)$$

$$T_{j0} = \frac{\left(\rho c_w (T_{jin} F_j + T_{in} F) + E_r\right) \cdot UA + \rho^2 c_w^2 F F_j T_{jin}}{\rho c_w (F_j + F) UA + \rho^2 c_w^2 F F_j}, \quad (6)$$

The value of the UA=5.67[kJ/min/K] parameter is obtained by minimizing the sum of squared differences between the model outputs (5)-(6) and the measured temperatures $\hat{T}$, $\hat{T}_j$ at N=31 steady-state conditions:

$$f(UA) = \sum_{i=1}^{N} (\hat{T}_i - T_{0i})^2 + \sum_{i=1}^{N} (\hat{T}_{ji} - T_{j0i})^2, \quad (7)$$

A part of the model 1, i.e., the equations (1)-(2) describing the heat transfer phenomena in the real hybrid reactor has been verified against the measurement data (Fig.2-3). In order to evaluate the accuracy of the model 1, the following error was defined and calculated:

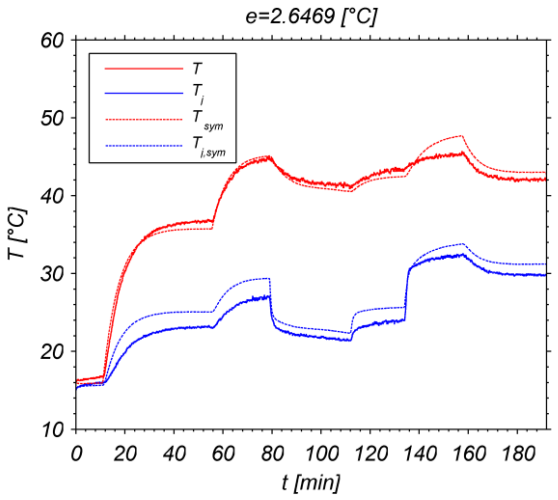

Fig. 2. Verification result for model 1 with UA=5.67[kJ/min/K]

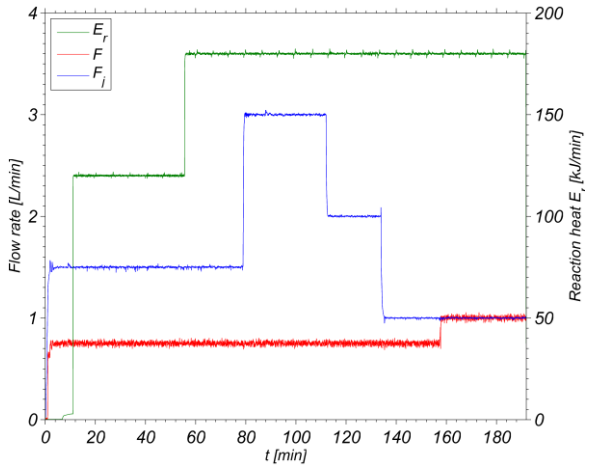

Fig. 3. Time evolution of flow rates F, F_j and energy E_r durring reference experiment (Fig. 2) used for verification.

$$e = \sqrt{\frac{1}{M}\sum_{i=1}^{M}\left(T_i - T_{sym,i}\right)^2} + \sqrt{\frac{1}{M}\sum_{i=1}^{M}\left(T_{j,i} - T_{jsym,i}\right)^2}, \quad (8)$$

where M is the number of time series samples in experimental data set. The value of the modeling error e is displayed above each figure presenting time courses of temperatures inside the reactor vessel and the jacket (Fig.2). During the verification experiments, the model (1)-(2) was simulated and excited by the same inputs T_{in}, T_{jin}, F, F_j and E_r as the real system.

One of the most significant uncertainties in the heat balance-based models are uncertainties related to heat losses. It is possible to evaluate the heat losses based on the total energy balance and experimental data obtained for different steady-states conditions. By setting the derivatives in (1) and (2) equal to zero, the total heat flow P_{HL} to the environment (due to heat losses) in steady-state can be estimated as follows:

$$P_{HL} = E_{r0} + c_p \rho F_0 (T_{in0} - T_0) + c_p \rho F_{j0} (T_{jin0} - T_{j0}), \quad (9)$$

where the additional index 0 denotes the steady-state conditions. The evaluated heat flows P_{HL} for various steady-states ranges between -7 [kJ/min] and 25 [kJ/min]. Negative value of P_{HL} was obtained for cases in which T_j temperature was lower than ambient one. A comparison of the maximum heating power of the electric heater (P_{max}=180[kJ/min]) with the heat flows P_{HL} shows that the heat transfer to the environment cannot be neglected in the mathematical model, especially for higher output temperatures. This results give general information only, but indicate that heat exchange with the ambient must be incorporated in the model. Because it is not known how much heat is transferred to the ambient air from the reactor vessel and from the jacket, it was assumed that heat exchange with the ambient are present in both these parts of the hybrid reactor. Hence, a modified form of the model 1 is:

$$c_p \rho V \frac{dT}{dt} = c_p \rho F (T_{in} - T) - UA (T - T_j) + E_r - Q_{na}, \quad (10)$$

$$c_p \rho V_j \frac{dT_j}{dt} = c_p \rho F_j (T_{jin} - T_j) + UA(T - T_j) - Q_{ja}, \quad (11)$$

where $Q_{ra}=UA_{ra}(T-T_a)$ and $Q_{ja}=UA_{ja}(T_j-T_a)$ are heat flows from the reactor vessel and the jacket to the ambient air, respectively. The model (10)-(11) will be referred to as the model 2.

Now the unknown parameters are UA, UA_{ra}, UA_{ja} and they can be estimated in the same way as for the model 1. By setting derivatives in (10) and (11) equal to zero, it is possible to find steady-state temperatures T_0 and T_{j0}, and then to minimize the objective function (7), which is now dependent on the three unknown parameters. For that purpose the same experimental data set was used and the identified parameter values are: UA=4.68[kJ/min/K], UA_{ra}=0.60[kJ/min/K] and UA_{ja}=0.13 [kJ/min/K]. By using UA_{ra} and UA_{ja} parameters it is possible to estimate the heat flow P_{HLa} to the environment:

$$P_{HLa} = UA_{ra} \cdot (T_0 - T_{a0}) + UA_{ja} \cdot (T_{j0} - T_{a0}) \quad (12)$$

The obtained heat flows P_{HLa} are compared with (9) and shown in Fig. 4. The higher the accuracy of the model (12), the smaller are the deviations from the diagonal line (Fig. 4). In turn, Fig.5 presents validation of the model 2 with the identified parameters UA, UA_{ra}, UA_{ja}, and for the same measurement data set as for the model 1. Although, the modeling error (8) is smaller than the error obtained for the model 1, there are still significant deviations between the measured and simulated temperatures. In order to find a more accurate description, the model 2 can be modified by introducing to its structure some empirical relations. A detailed analysis of the obtained results can give us a simple relation for the UA parameter as a function of F_j and T_j variables. The relation for the UA should be as simple as possible, and at the same time, ensuring a better accuracy of the dynamical model of the hybrid reactor. The model with variable UA coefficient is not built to explain all the phenomena in the process, but to increase its accuracy. One of the simplest forms of the function

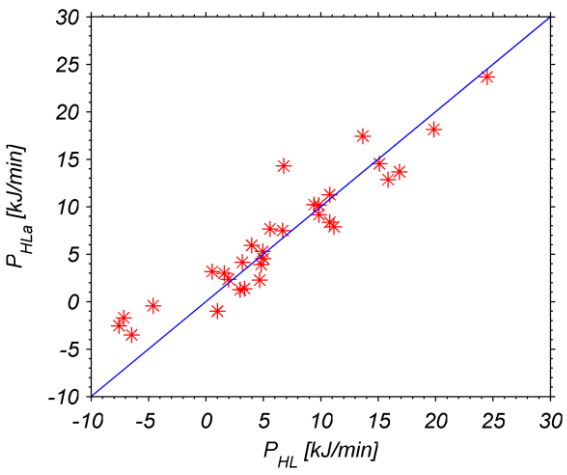

Fig. 4. Approximation result of heat exchange with the ambient. Horizontal axis represents values obtained on the total energy balance (9). Vertical axis represent values obtained on the base of aproximation (12).

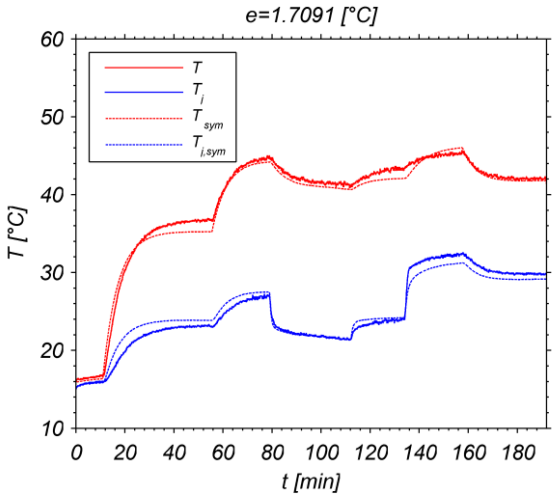

Fig. 5. Verification result for model 2 with UA=4.68[kJ/min/K], UA_{ra}=0.60[kJ/min/K], UA_{ja}=0.13[kJ/min/K]

$UA=UA(F_{j0},T_{j0})$ is an affine function that cannot be derived by using physical laws, but results from our observations:

$$UA = p_0 + p_1 \cdot F_j + p_2 \cdot T_j, \quad (13)$$

where p_0=-55.88, p_1=0.73, p_2=0.20. The parameter values in (13) were obtained by using Matlab curve fitting tool (*cftool* function). The other parameter values are the same as for the model 2. The model (10)-(11) with the variable UA (13) will be referred to as the model 3. Fig.6 presents the validation results for the model 3 using the same data set as for the models 1 and 2. The modeling error (8) is given above Fig. 6.

As can be clearly seen, the modeling error is smaller and a better accuracy of the model is obtained. The variable UA coefficient (13) had also an impact on the steady-state temperature values. The obtained results (Fig.6) has shown that the model 1 or model 2 was too simple to capture the steady-state state and dynamical behavior of the hybrid reactor.

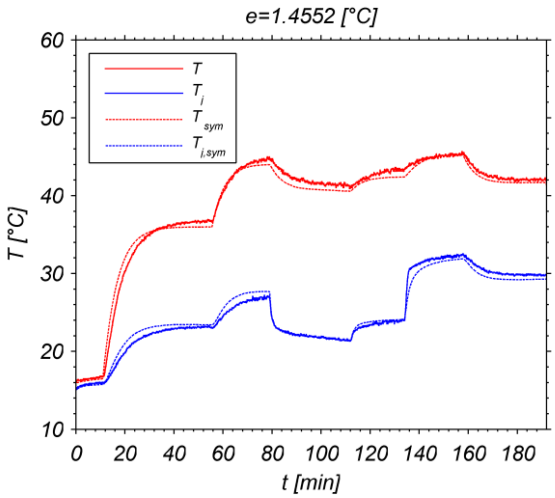

Fig. 6. Verification result for the model 3 with with variable UA coefficient and UA_{ra}=0.60[kJ/min/K], UA_{ja}=0.13[kJ/min/K]

Moreover, variations in the *UA* coefficient may suggest that the reactor content and coolant in the jacket are not well-mixed, as assumed at the beginning of this study. Because the classical CSTR system (1)-(4) exhibits multiplicity of steady-states and oscillatory behavior, it is especially interesting how the variable *UA* coefficient influences the presence of hysteresis, oscillations and stability of the process. Further results will show the dynamical behavior of the models 1, 2 and 3 with additional equation (3) and it is assumed that $E_r=(-\Delta H)\cdot V\cdot r$, where the reaction rate r is given by (4).

IV. Bifurcation Analysis of the Hybrid Reactor

By including heat transfer to the environment (due to heat losses) and additional equation (13), it was possible to increase the accuracy of the mathematical model of the hybrid reactor. However, the modification of the model can also affect its dynamical behavior [30], i.e., depending on the flow rates F and F_j. To analyze the dynamical behavior of the CSTR system, we have performed the bifurcation analysis of the models 1, 2 and 3 by using XPPAut software [31]. The flow rate F_j was chosen as a bifurcation parameter, since this parameter is often chosen as the manipulating variable in the design of control system for the CSTR.

Fig. 7 presents the steady-state temperature inside the reactor vessel for various flow rates F_j. The continuous lines represent stable branches and the broken lines are unstable ones. The stability was determined in XPPAut based on the eigenvalues of the linearized system [31]. In each case, the hybrid reactor system is unstable for some range of flow rates F_j and exhibits the oscillatory behavior. The rectangle symbols represents the Hopf points that correspond to the case in which a pair of purely imaginary eigenvalues of the linearized system crosses the imaginary axis. In effect, one can observe the oscillations of state variables. It should be noted that these oscillations appear for smaller flow rates F_j for models 2 and 3 in comparison to the behavior of the classical CSTR (model 1) for the same flow rate F=0.2[L/min].

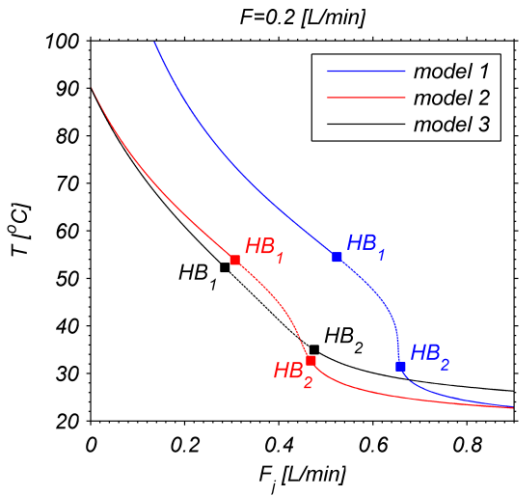

Fig. 7. Bifurcation diagrams for hybrid reactor systems showing the steady-state temperature inside the reactor vessel as flow rate F_j varies for F=0.2[L/min]; HB stands for Hopf bifurcation.

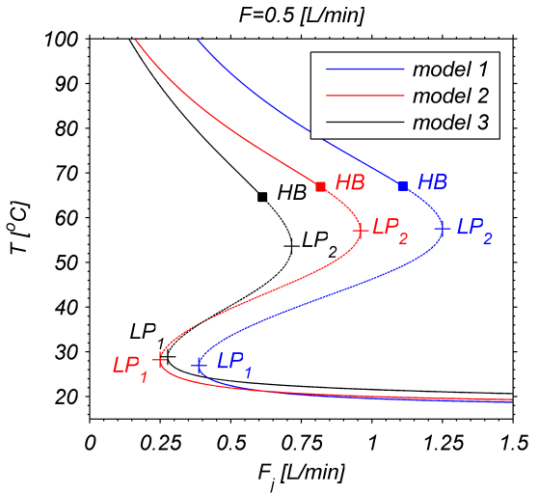

Fig. 8. Bifurcation diagrams for hybrid reactor systems showing the steady-state temperature inside the reactor vessel as flow rate F_j varies for F=0.5[L/min]; LP stands for limit point (saddle-node bifurcation).

Further analysis on the parameter plane (F_j,F) has shown that the region of oscillatory behavior is also shifted towards smaller values of F_j for various flow rates F and the results for F=0.5[L/min] have been shown in Fig. 8. Irrespective of the model complexity each system exhibited the hysteresis effect and oscillatory behavior in a narrow range of flow rates F_j. In comparison to the classical CSTR system, the hysteresis effect is smaller for the systems with heat losses and variable *UA* coefficient. This can be explained by analyzing equilibrium points for models without (model 1) and with heat losses (model 2) to the environment.

By setting the derivatives in (1)-(3) and in (10)-(11) equal to zero, one can find the equilibrium points by using a graphical method, i.e., by analyzing the number of intersections of a sigmoid line (black line in Fig.9) representing the production of the reaction heat with a straight line representing the heat flow removed from the system (Fig. 9). The slope of the straight

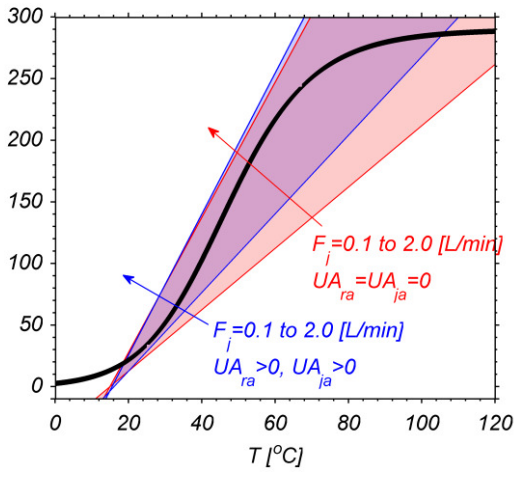

Fig. 9. The graphical analysis of the number of equilibrium points for the classical CSTR (model 1) and model 2 for F=0.5[L/min] and various flow rates F_j. Depending on the flow rate F_j, the straight lines are located within the blue and red sectors.

lines (blue and red ones in Fig.9) can vary depending on the flow rate F_j and a common intersection point is for $T=T_{jin}$ (model 1) or for $T=T_{jin}(1+UA_{ja}/UA)-T_a \cdot UA_{ja}/UA$ (model 2). By changing the flow F_j in the same range (from 0.1 to 2.0[L/min]), it is easily to show that the slope of the straight line is greater for the system with heat losses (model 2). As a result, the hysteresis effect appears for smaller flow rates F_j in comparison to the classical CSTR system (Fig. 9). This is a consequence of the fact that the reaction heat is partially removed to the environment due to heat losses. Therefore, in the real system one should expect the hysteresis effect for smaller values of F_j. The analysis of the system with the heat loss and variable *UA* coefficient (model 3) is more complex and the numerical results obtained for this case are presented in Fig. 7 and Fig. 8.

V. CONCLUSIUONS

The obtained results has shown that the classical CSTR model is not sufficient to describe the static and dynamical behavior of the real hybrid reactor system. The modeling error was reduced for the model with additional terms for the heat transfer to the ambient air. Further reduction of the modeling error was possible for the model with variable *UA* coefficient. It was assumed that the *UA* coefficient was strictly dependent on the flow rate F_j and the temperature T_j inside the reactor jacket. This suggest that temperature distribution inside the reactor vessel and jacket may not be uniform and further studies on this subject are needed. In turn, bifurcation analysis of the models has shown that the model with variable *UA* coefficient exhibits qualitatively the same dynamical behavior as the classical CSTR system.

ACKNOWLEDGMENT

This work was supported by the Ministry of Science and Higher Education under grant BKM/506/RAU1/2016

REFERENCES

[1] R. Aris and N. Amundson, “An analysis of chemical reactor stability and control,” Chem. Engng. Sci., vol. 7, pp. 121-155, 1958.

[2] D.E. Seborg, T.F. Edgar and D.A. Mellichamp, Process Dynamics and Control. Wiley Series in Chemical Engineering, 1989.

[3] W.L. Luyben, Process Modeling, Simulation and Control for Chemical Engineers. McGrawHill, 1990.

[4] M.A. Henson and D.E. Seborg (ed.), Nonlinear Process Control, Upper Saddle River, Prentice Hall PTR, 1997.

[5] J.B. Riggs, and R.R. Rhinehart “Comparison between two nonlinear process-model based controllers,” Comput. chem. Engng., vol. 14, pp. 1075-1081, October 1990.

[6] R.R. Rhinehart, “Model-based control,” in: Instrument Engineers Handbook (B.G. Liptak – Ed.), Taylor and Francis, CRC Press, Boca Raton, FL, 2005.

[7] A. Isidori, Nonlinear Control Systems. Springer Verlag, New York, 1989.

[8] M.A. Henson and D.E. Seborg “Input-output linearization of general nonlinear process,” AICHE J., vol. 36, pp. 1753-1757, November 1990.

[9] P.L. Lee and G.R. Sullivan, “Generic model control (GMC),” Comput. Chem. Engng., vol. 12, pp. 573-580, June 1988.

[10] J. Richalet, A. Rault, J.L. Testud and J. Papon, “Model predictive heuristic control: applications to industrial processes,” Automatica, vol. 14, pp. 413-418, September 1978.

[11] J. Richalet and D. O’Donovan, Predictive Functional Control, Springer, London 2009.

[12] P. Laszczyk, “Predictive control library block for Simatic-S7 PLC,” in PdeS’2006 Preprints of IFAC Workshop On Programmable Devices And Embedded Systems, Brno, Czech Republic, February 2006.

[13] G. Valencia-Palomo and J.A. Rossiter, “Programmable logic controller implementation of an auto-tuned predictive control based on minimal plant information,” ISA T., vol. 50, pp. 92-100, January 2011.

[14] T. Klopot, K. Stebel, J. Czeczot, and P. Laszczyk, “Function block practical implentation of Balance-Based Adaptive Control for pH process,” in: 39th Annual Conference of the IEEE Industrial Electronics Society, IECON 2013, Vienna, Austria, pp. 3547–3552.

[15] T. Klopot, P. Laszczyk, K. Stebel and J. Czeczot, “Flexible function block implementation of the balance-based adaptive controller as the potential alternative for PID-based industrial applications,”, T. I. Meas. Control, vol. 36, pp. 1098-1113, December 2014.

[16] T. Klopot, P. Skupin, D. Choinski, R. Cupek, M. Fojcik, "A metamorphic controller for plant control system design," Model. Identif. Control, vol. 37, pp. 159-169, March 2016.

[17] K. Huang and B. Lu, “The precise condition of thermal runaway in microwave heating on chemical reaction,” Science in China Series E: Technological Sciences, vol. 52, pp. 491-496, February 2009.

[18] M. Niedzwiedz and P. Laszczyk, “Probe dynamics influence on determination of volumetric oxygen transfer coefficient,” in: 19th International Conference on Methods and Models in Automation and Robotics (MMAR), pp. 395-400, 2014.

[19] T. Weber and P. Harriot, “Control of a continuous-flow agitated-tank reactor,” Ind. Eng. Chem. Fund., vol. 4, pp. 264-269, August 1965.

[20] M.R. Juba and J.W. Hammer, “Progress and challenges in batch process control,” in Proceedings of the Chemical Process Control (CPC '86), vol. 3, pp. 139–183, Elsevier, 1986.

[21] L.S. Kershenbaum and P. Kittisupakorn, “The use of a partially simulated exothermic (PARSEX) reactor for experimental testing of control algorithms,” Chem. Eng. Res. Des., vol. 72, pp. 55-63, January 1994.

[22] P. Afonso, N. Oliveira and J. Castro, “Model predictive control of a pilot plant reactor with a simulated exothermic reaction,” Comput. Chem. Eng., vol. 20, pp. S769-S774, May 1996.

[23] N.F. Thornhill, S.C. Patwardhan and S.L. Shah, “A continuous stirred tank heater simulation model with applications,” J. Proc. Contr., vol. 18, pp. 347-360, March 2008.

[24] K.S. Lee, I.S. Chin, H.J. Lee and J.H. Lee, “Model predictive control technique combined with iterative learning for batch processes”, AICHE J. , vol. 45, pp. 2175-2187, October 1999.

[25] M. Metzger, “Easy programmable controller for hybrid exothermic reactor,” in Preprints of the IFAC Workshop on Programmable Devices and Systems, Elsevier, Ostrava, pp. 69-74, February 2003.

[26] M. Mezghani, G. Roux, M. Cabassud, M.V. Le Lann, B. Dahhou and G. Casamatta, “Application of iterative learning control to an exothermic semibatch chemical reactor”, IEEE T. Contr. Syst. T., vol. 10, pp. 822-834, November 2002.

[27] J. Cueli and C. Bordons, “Iterative nonlinear model predictive control. stability, robustness and applications,” Control Eng. Pract., vol. 16, pp. 1023-1034, September 2008.

[28] C. Pinheiro, and L. Kershenbaum, “Model predictive control of reactor temperature in a CSTR pilot plant operating at an unstable steady-state,” Comput. Chem. Eng., vol. 23, pp. S859-S862, June 1999.

[29] L.O. Santos, P.A. Afonso, J.A. Castro, N.M. Oliveira, and L.T. Biegler, “On-line implementation of nonlinear MPC: an experimental case study,” Control Eng. Pract., vol. 9, pp. 847-857, August 2001.

[30] Y.S. Chien, "The effect of non‐ideal mixing on the number of steady states and dynamic behaviour for autocatalytical reactions in a CSTR," Can. J. Chem. Eng., vol. 79, pp. 112-118, February 2001.

[31] B. Ermentrout, Simulating, Analyzing, and Animating Dynamical Systems. A Guide to XPPAUT for Researchers and Students, SIAM series Software Environments and Tools, Philadelphia PA, 2002.